

# Bayesian Inference for Stationary Points in Gaussian Process Regression Models for Event-Related Potentials Analysis

Cheng-Han Yu<sup>1</sup>, Meng Li<sup>1</sup>, Colin Noe<sup>2</sup>, Simon Fischer-Baum<sup>2</sup> and Marina Vannucci<sup>1</sup>

<sup>1</sup>Department of Statistics, Rice University, Houston, TX, USA

<sup>2</sup>Department of Psychological Science, Rice University, Houston, TX 77005.

\**email*: marina@rice.edu

**SUMMARY:** Stationary points embedded in the derivatives are often critical for a model to be interpretable and may be considered as key features of interest in many applications. We propose a semiparametric Bayesian model to efficiently infer the locations of stationary points of a nonparametric function, while treating the function itself as a nuisance parameter. We use Gaussian processes as a flexible prior for the underlying function and impose derivative constraints to control the function's shape via conditioning. We develop an inferential strategy that intentionally restricts estimation to the case of at least one stationary point, bypassing possible mis-specifications in the number of stationary points and avoiding the varying dimension problem that often brings in computational complexity. We illustrate the proposed methods using simulations and then apply the method to the estimation of event-related potentials (ERP) derived from electroencephalography (EEG) signals. We show how the proposed method automatically identifies characteristic components and their latencies at the individual level, which avoids the excessive averaging across subjects which is routinely done in the field to obtain smooth curves. By applying this approach to EEG data collected from younger and older adults during a speech perception task, we are able to demonstrate how the time course of speech perception processes change with age.

**KEY WORDS:** Bayesian inference; Semiparametric; Gaussian process; Derivatives; ERP data.

## 1. Introduction

Shape constraints in the form of stationary points embedded in the derivatives arise naturally in a wide range of modern applications. Estimation of the stationary points of functional curves, in addition to the fitted curves, may be considered key features of interest in many applications. In our motivating example, event-related potentials (ERPs) are derived by averaging electroencephalography (EEG) signals, collected in response to specific stimuli or events, and used to infer brain electrical potentials (Gasser and Molinari, 1996). ERP waveforms consist of characteristic components that span across time, and that relate to specific mental or cognitive processes, such as signal matching, decision making, language processing and memory updating (Luck, 2012). Analyses of ERP data often focus on identifying the amplitude (magnitude of the peak) and latency (time when the peak or dip occurs) of specifically meaningful peaks or characteristic components (Luck, 2005). The two most common methods are hand selecting peaks or integrating the area under the curve over a pre-set time-window and these methods have remained largely unchanged over the past fifty years, see Luck (2012). In recent years, some alternative approaches have been proposed for detecting ERPs in single subjects, such as those based on the studentized continuous wavelet transformation technique, see for example Kallionp et al. (2019) for discussion and a comparison of these techniques. However, these methods are typically designed to detect whether or not an ERP component is present, either for the development of brain-computer interface devices or for assessment of clinical characteristics, such as the persons state of consciousness. This research therefore differs from the goal of our work, which is to provide reliable estimations of ERP curve features, including the latency and amplitude, at the single subject level. In statistics, there has been a limited literature to analyze ERP data; a notable exception is Hasenstab et al. (2015) where a moving average-based meta-preprocessing procedure was proposed to increase the signal-to-noise ratio, which was used

to identify longitudinal trends and adopted by Hasenstab et al. (2017). Our focus is instead on detecting stationary points under noisy ERP data.

In this paper, we propose a semiparametric Bayesian model to efficiently infer the locations of stationary points of a nonparametric function, while treating the function itself as a nuisance parameter. Specifically, we use Gaussian processes (GPs) as a flexible prior for the underlying function and impose derivative constraints to control the function's shape. This leads to a new process bearing a particular form of GPs, which is referred to as *Derivative-constrained GP*, as it incorporates derivative constraints via conditioning. GPs have been arguably one of the most widely used nonparametric processes for continuous curves in Bayesian statistics and machine learning, partly due to their flexibility and tractability, see Rasmussen and Williams (2006) and Ghosal and van der Vaart (2017) for a comprehensive treatment. Holsclaw et al. (2013) estimates the derivative of a curve using GP based inverse method, avoiding direct estimation from the data through differentiation of the covariance function. Zhou et al. (2019) uses constrained Gaussian processes to enforce constraints on the parameter space such as convexity and inequality of linear combinations through indicator functions. Wang and Berger (2016) studies various strategies including constrained Gaussian processes and conditional Gaussian processes by conditioning a unrestricted Gaussian process on a positive probability event. While the emphasis in the majority of these approaches is to investigate the benefit of adding shape constraints to the fitting of the original function, in this paper we are primarily interested in the estimation of the stationary points of the underlying function. In addition, our approach utilizes the desirable property that the derivative of a GP, along with the original sample path, is also jointly a GP, provided that the GP is mean-square differentiable, see for example Ch. 2 of Adler (1981).

In our application to EEG data, the derivative constraints are only partially specified, that is, the prior knowledge is only concerned with the existence of finitely many stationary

points, while their number and locations are left unknown. We adopt the conditioning approach by unifying the curve fitting and stationary points detection, which is presumably more suited for extremely low signal-to-noise ratio data such as EEG. This allows us to intentionally restrict estimation to the case of *at least one stationary point*, bypassing possible mis-specifications in the number of stationary points and avoiding the varying dimension problem that often brings in computational complexity. For posterior inference, we propose a stochastic EM algorithm that allows uncertainty quantification on the number and locations of the stationary points. We illustrate the proposed methods using simulations and then apply the method to the estimation of ERP data derived from EEG signals, where we show how the proposed method can be employed to estimate smooth curves and automatically identify characteristic components and their latencies through the detection of the stationary points of the curves. By applying our approach to data collected from younger and older adults during a speech perception task, we are able to demonstrate how the time course of speech perception processes change with age. Unlike exploratory methods that rely on visual inspection of the curves, our method provides uncertainty quantification on the estimated quantities via high posterior density regions. Furthermore, by explicitly accounting for error in the data, we avoid the excessive averaging which is routinely done to obtain smooth curves. This provides a major advance over the standard approaches in the clinical and cognitive literature for how single-subject ERP components latency and amplitude are estimated. The clinical and scientific need for more reliable single-subject measures is clear, as there is increasing interest in relating individual differences in ERP components to individual differences in behavior, both for answering theoretical questions (Kim et al., 2018; Tanner, 2019) and clinical uses (Hajcak et al., 2019). Our work lays the foundation for more sophisticated statistical models for ERP data that can produce more reliable estimations of ERP curve features, including amplitude and latency.

The rest of the article is organized as follows. Section 2 presents the proposed model, the GP prior construction and the stochastic EM algorithm for posterior inference. Section 3 examines the performance of the proposed method via simulations, Section 4 presents the ERP case study, followed by discussion and conclusions in Section 5.

## 2. Methods

### 2.1 Shape-constrained regression

Let  $\mathbf{y} = \{y_1, \dots, y_n\}$  be noisy observations from an unknown function  $f : \mathcal{X} \rightarrow \mathbb{R}$  observed at locations  $\mathbf{x} = \{x_1, \dots, x_n\}$ . We assume a nonparametric regression model of the type

$$y_i = f(x_i) + \epsilon_i, \quad i = 1, \dots, n, \quad (1)$$

where  $\epsilon_i$  is Gaussian random noise, i.e.,  $\epsilon_i \stackrel{\text{iid}}{\sim} N(0, \sigma^2)$ . We are interested in situations where  $f(\cdot)$  has  $M$  stationary points,

$$f'(t_m) = 0, \quad m = 1, \dots, M, \quad (2)$$

with  $f'(\cdot)$  indicating the first derivative of  $f(\cdot)$ . Model construction (1) - (2) extends the classic nonparametric regression model to incorporate derivative constraints on the unknown flexible regression function. The stationary points  $\mathbf{t} = (t_1, \dots, t_M)$  in (2), which may or may not coincide with the input values in (1), are our parameters of interest, while the underlying function  $f(\cdot)$  is a nuisance parameter. One primary objective is to estimate the number of stationary points  $M$  if it is unknown and their locations  $\mathbf{t}$ . Below we propose a novel Bayesian method to fit the model and carry out statistical inference. In particular, we use derivative-constrained Gaussian processes (DGP) to incorporate the shape constraints on  $f(\cdot)$  and intentionally restrict to the case of *at least one stationary point* to bypass the possible misspecification of  $M$  if it is unknown and avoid the varying dimension of  $\mathbf{t}$  that often brings in computational complexity. We also derive inferential tools to quantify the uncertainties in the estimation of  $\mathbf{t}$ .

## 2.2 Derivative-constrained Gaussian processes (DGP)

We model the unknown function  $f(\cdot)$  via a Gaussian process prior

$$f(\cdot) \sim GP(\mu(\cdot), k(\cdot, \cdot)), \quad (3)$$

with constant mean function, i.e.,  $\mu(\cdot) = \mathbf{E}(f(x_i)) = \mu$ , and covariance function  $k(x_i, x_j) = \text{cov}(f(x_i), f(x_j))$  (Rasmussen and Williams, 2006). For concreteness, we focus here on  $\mathcal{X} = [a, b]$  and notice that the proposed methods are readily applicable for general domains such as  $\mathcal{X} = [a, b]^d$  for  $d \geq 1$ . It is well known that a Gaussian process possesses a version whose sample paths are differentiable if its covariance kernel is continuously differentiable (Ghosal and van der Vaart, 2017, page 574); throughout this paper, we always refer to such differentiable sample paths for a Gaussian process. Since differentiation is a linear operator, the derivative of a Gaussian process is also a Gaussian process. This desirable property makes Gaussian processes well suited for our purpose to study the location of the stationary points when the true function is unknown.

In the sequel we indicate with  $W = \{W_x, x \in \mathcal{X}\}$  a differentiable sample path of  $GP(\mu(\cdot), k(\cdot, \cdot))$ .

Given two arbitrary points  $(x, \tilde{x})$  from  $\mathcal{X}$ , we have (Parzen, 1962)

$$\begin{aligned} \text{cov}(W'_{\tilde{x}}, W_x) &= \frac{\partial}{\partial \tilde{x}} \text{cov}(W_{\tilde{x}}, W_x) = \frac{\partial}{\partial \tilde{x}} k(\tilde{x}, x) := k_{10}(\tilde{x}, x) \\ \text{cov}(W_x, W'_{\tilde{x}}) &= \frac{\partial}{\partial \tilde{x}} \text{cov}(W_x, W_{\tilde{x}}) = \frac{\partial}{\partial \tilde{x}} k(x, \tilde{x}) := k_{01}(x, \tilde{x}) = k_{10}(\tilde{x}, x) \\ \text{cov}(W'_x, W'_{\tilde{x}}) &= \frac{\partial^2}{\partial x \partial \tilde{x}} \text{cov}(W_x, W_{\tilde{x}}) = \frac{\partial^2}{\partial x \partial \tilde{x}} k(x, \tilde{x}) := k_{11}(x, \tilde{x}). \end{aligned}$$

Extending the derivative operation to two arbitrary vectors  $\mathbf{x} = (x_1, \dots, x_J)$  and  $\tilde{\mathbf{x}} = (\tilde{x}_1, \dots, \tilde{x}_J)$  yields a random vector  $(W_{x_1}, \dots, W_{x_J}, W'_{\tilde{x}_1}, \dots, W'_{\tilde{x}_J})$  which is distributed according to a multivariate normal distribution with mean  $(\mu(\mathbf{x})^T, \mu'(\tilde{\mathbf{x}})^T)^T$  and covariance

$$\begin{bmatrix} k(\mathbf{x}, \mathbf{x}) & k_{01}(\tilde{\mathbf{x}}, \mathbf{x}) \\ k_{01}(\mathbf{x}, \tilde{\mathbf{x}}) & k_{11}(\tilde{\mathbf{x}}, \tilde{\mathbf{x}}) \end{bmatrix},$$

where we adopt the shorthand  $\mu(\mathbf{x})$  to denote the vector  $(\mu(x_1), \dots, \mu(x_J))$ ,  $k_{10}(\tilde{\mathbf{x}}, \mathbf{x})$  to denote the matrix whose  $ij$ th entry is  $k_{10}(\tilde{x}_i, x_j)$ , with the same convention for  $\mu'(\tilde{\mathbf{x}})$ ,  $k(\mathbf{x}, \mathbf{x})$ ,

$k_{01}(\mathbf{x}, \tilde{\mathbf{x}})$ , and  $k_{11}(\tilde{\mathbf{x}}, \tilde{\mathbf{x}})$ . Consequently, the conditional distribution of  $(W_{x_1}, \dots, W_{x_j})$  given  $(W'_{\tilde{x}_1}, \dots, W'_{\tilde{x}_j}) = \mathbf{0}$  is a multivariate normal with mean  $[\mu(\mathbf{x}) - k_{01}(\mathbf{x}, \tilde{\mathbf{x}})k_{11}^{-1}(\tilde{\mathbf{x}}, \tilde{\mathbf{x}})\mu'(\tilde{\mathbf{x}})]$  and covariance  $[k(\mathbf{x}, \mathbf{x}) - k_{01}(\mathbf{x}, \tilde{\mathbf{x}})k_{11}^{-1}(\tilde{\mathbf{x}}, \tilde{\mathbf{x}})k_{10}(\tilde{\mathbf{x}}, \mathbf{x})]$ . This leads to the following definition of a Gaussian process with derivative constraints at stationary points  $\mathbf{t} = (t_1, \dots, t_M)$ .

**DEFINITION 1:** A random process  $W$  is said to be a derivative-constrained Gaussian process at points  $\mathbf{t}$ , denoted by  $\text{DGP}(\mu, k, \mathbf{t})$ , if it follows a Gaussian process with mean function  $x \mapsto \mu(x) - k_{01}(x, \mathbf{t})k_{11}^{-1}(\mathbf{t}, \mathbf{t})\mu'(\mathbf{t})$  and covariance kernel  $(x, \tilde{x}) \mapsto [k(x, \tilde{x}) - k_{01}(x, \mathbf{t})k_{11}^{-1}(\mathbf{t}, \mathbf{t})k_{10}(\mathbf{t}, \tilde{x})]$ .

It is easy to see that the sample paths of a  $\text{DGP}(\mu, k, \mathbf{t})$  have zero derivatives at  $\mathbf{t}$  almost surely. We note that, unlike most conditional GPs used in the literature, the conditioning event in our DGP has zero probability and involves unknown parameters. In the sequel, we use a *squared exponential* (SE) Gaussian process, with kernel

$$k(x_i, x_j) = \tau^2 \exp\left(-\frac{1}{2h^2}\|x_i - x_j\|^2\right), \quad (4)$$

which is infinitely differentiable. The parameter  $\tau^2$  controls the vertical variation of the process, and  $h$  is the so called length scale parameter that controls the correlation range of the process. A larger  $h$  results in higher correlation between inputs and ends up with a smoother curve. The induced DGP is defined based on the partial derivatives of  $k(\cdot, \cdot)$ :

$$\begin{aligned} k_{01}(x_i, t_j) &= k_{10}(t_j, x_i) = \tau^2 \exp\left(-\frac{1}{2h^2}|x_i - t_j|^2\right) \frac{(x_i - t_j)}{h^2}, \\ k_{11}(t_i, t_j) &= \tau^2 \exp\left(-\frac{1}{2h^2}|t_i - t_j|^2\right) \left(\frac{1}{h^2} \left(1 - \frac{(t_i - t_j)^2}{h^2}\right)\right). \end{aligned}$$

Other kernels with required differentiability can also be used; see (Rasmussen and Williams, 2006, Ch 4) for a detailed discussion of covariance functions. Figure 1 shows some sample paths a Gaussian process, obtained with the SE kernel (4) and parameters  $\tau = 1$  and  $h = 1$ , with and without derivatives constraints. It is important to notice that imposing derivative constraints on  $M$  points implies that every GP path will have *at least*  $M$  stationary points. Below we exploit this simple fact when imposing priors on the stationary points.

[Figure 1 about here.]

### 2.3 Priors on stationary points

Let's consider model (1) - (2), with the GP prior (3) on  $f$ . A standard strategy to specify the prior  $\pi(\mathbf{t})$  on the stationary points is to specify a hierarchical distribution through an  $M$ -dimensional prior for  $\mathbf{t}$  supported on  $\mathcal{X}^M$ , with a hyperprior on  $M$ . We refer to this strategy as *multiple-DGP*. Alternatively, we propose to use a univariate stationary point  $t$  with a prior  $\pi(t)$  supported on  $\mathcal{X}$ , which corresponds to assuming that the regression function has *at least one* stationary point, and then utilize the posterior of  $t$  to infer all stationary points. We refer to this strategy as *single-DGP*. Multiple-DGP inevitably involves a varying dimension of  $\mathbf{t}$  in the posterior sampling and model selection for various values of  $M$ . Although a reversible jump MCMC can be used for sampling purposes, misspecification of  $M$  might exert substantive effects on the posterior inference of  $\mathbf{t}$  when the sample size is finite. In contrast, single-DGP bypasses such concerns essentially relying on a multi-modal posterior of  $t$ . To support this claim, in Section 3 and in the Supplementary Material we compare the two strategies on simulated data and real data and recommend single-DGP for practical applications of our method.

### 2.4 Posterior inference via stochastic EM

Let  $\boldsymbol{\theta} = (\sigma, \tau, h)$  indicate all model parameters other than  $\mathbf{t}$ . Without the derivative constraints, one popular method to estimate  $\boldsymbol{\theta}$  is to calculate empirical Bayes (EB) estimates by maximizing the marginal log-likelihood of  $\boldsymbol{\theta}$ , which is a multivariate normal density. A flat or noninformative prior on  $\boldsymbol{\theta}$  is typically assumed. For the proposed single-DGP model, we develop a stochastic expectation-maximization (SEM) algorithm for posterior inference, which includes hyperparameter selection. The proposed SEM algorithm draws samples of stationary points based on one posterior estimate of  $\boldsymbol{\theta}$  in the E-step, either by rejection sampling or Metropolis-Hastings algorithm (Hastings, 1970), and calculates the



maximum a posteriori (MAP) estimate of  $\boldsymbol{\theta}$  in the M-step by maximizing the posterior distribution calculated over the stochastic stationary points. The algorithm is summarized below. Convergence is reached when  $\|\boldsymbol{\theta}^{(i+1)} - \boldsymbol{\theta}^{(i)}\| < \epsilon$  at the  $(i + 1)$ -th iteration. Here we use  $\epsilon = 0.0001$  as the tolerance level.

---

**Algorithm 1:** Stochastic EM Algorithm for single-DGP

---

Set initial value  $\hat{\boldsymbol{\theta}}^{(1)}$ , for example from a  $U(a, b)$ .

For iteration  $i = 1, 2, \dots$  until convergence criterion  $\|\hat{\boldsymbol{\theta}}^{(i)} - \hat{\boldsymbol{\theta}}^{(i+1)}\| < \epsilon$  is satisfied:

**Stochastic E-step:** Sample  $\{t_d^{(i)}\}_{d=1}^D$  from  $p(t | \mathbf{y}, \hat{\boldsymbol{\theta}}^{(i)}) \propto p(\mathbf{y} | t, \hat{\boldsymbol{\theta}}^{(i)})\pi(t)$ , either by Metropolis-Hastings or rejection sampling (with candidate proposal  $U(a, b)$  and constant  $M$  set to  $\arg \max_{t, \boldsymbol{\theta}} p(\mathbf{y} | t, \boldsymbol{\theta})$ ).

**if**  $i = 1$  **then**

$\{t_d^{(i)}\}_{d=1}^D \sim U[a, b]$ ;

**else**

**while**  $d \neq D$  **do**

$(t_d^{(i)})^* \sim q(t)$ ;

$u \sim U(0, 1)$ ;

**if**  $u < \pi((t_d^{(i)})^* | \mathbf{y}, \boldsymbol{\theta}^{(i)}) / M q((t_d^{(i)})^*)$  **then**

$t_d^{(i)} = (t_d^{(i)})^*$ ;

$d \leftarrow d + 1$

**end**

**end**

**end**

**M-step:** Given prior  $\pi(\boldsymbol{\theta})$  and samples of  $t$  at the  $i$ -th iteration,  $\{t_d^{(i)}\}_{d=1}^D$ , update  $\boldsymbol{\theta}$  to  $\hat{\boldsymbol{\theta}}^{(i+1)}$  by setting

$$\hat{\boldsymbol{\theta}}^{(i+1)} = \arg \max_{\boldsymbol{\theta}} \left[ \log \left[ \frac{1}{D} \sum_{d=1}^D p(\mathbf{y} | t_d^{(i)}, \boldsymbol{\theta}) \right] + \log \pi(\boldsymbol{\theta}) \right].$$

**Result:** MAP of  $\boldsymbol{\theta}$  and posterior samples of  $t$

---

### 3. Simulation Study

In this section, we examine the performance of our proposed model and stochastic EM algorithm through a simulation study. We consider a basic univariate response, with a one dimensional covariate  $x$ , and a nonlinear regression function of the type  $f(x) = (0.3 + 0.4x + 0.5 \sin(3.2x) + 1.1/(1 + x^2))$ , with  $x$  in  $\mathcal{X} = [0, 2]$  and two stationary points at  $t_1 = 0.436$

and  $t_2 = 1.459$ . We set  $n = 50$  and generate 100 independent data sets, according to model (1)-(2) with  $\sigma = 0.25$  and inputs  $\{x_i\}_{i=1}^n$  generated from a  $Unif(0, 2)$  distribution.

Results reported below were obtained by fitting DGP models with constant mean, that is  $\mu = 0$  without loss of generality, and SE covariance function (4). Data were centered prior to the analysis. As for the prior on  $\theta$ , we assumed  $\pi(\sigma^2, \tau^2, h) = \pi(\sigma^2)\pi(\tau^2)\pi(h)$  and imposed noninformative priors for  $\tau^2$  and  $h$ , i.e.,  $\pi(\tau^2) \propto 1$  and  $\pi(h) \propto 1$ , and a vague  $IG(1/2, 1/2)$  prior on  $\sigma^2$ . The SEM algorithm was used to obtain estimates of  $\theta$  and  $t$ . In the comparisons below we also fit a standard Gaussian process regression (GPR) model, where we employ an empirical Bayes approach to estimate  $\theta$ . We use the posterior means as the Bayes estimators unless stated otherwise. Although not of primary interest in our motivating data application, the estimation of the regression function is considered in the simulation to assess each method, where an equally-spaced test grid of length 100,  $\{x_j^*\}_{j=1}^{100}$ , is used for visualization and quantitative comparison.

### 3.1 Performance comparison

In evaluating the performance of our method, we consider the following three different settings. *Oracle-DGP* assumes that the number of stationary points and their locations are known and incorporated into the model via the constraint  $f'(0.436) = 0$  and  $f'(1.459) = 0$ . This scenario is unrealistic; however, we include it in our study to evaluate the improvement in estimating the regression function when such information is provided, with respect to a standard GPR model. The second setting is a simplified case of the *multiple-DGP* framework previously described, where we assume that one has prior knowledge about the number of stationary points and some knowledge about their locations. See Supplementary Material for a description of an adaptation of our stochastic EM Algorithm to this multiple-DGP framework. In particular, here we assume that  $t_1$  is in the interval  $(0, 1)$  and  $t_2$  in  $(0, 2)$ . We then assign prior distributions  $t_1 \sim Unif(0, 1)$  and  $t_2 \sim Unif(1, 2)$ . This scenario can be

problematic, particularly when the number of stationary points is over-specified since forcing zero derivatives when the true function is indeed not flat will result in distorted fitted curves. Moreover, with overlapping prior intervals, for example,  $t_1 \sim U(0, 1.5)$ ,  $t_2 \sim U(0.5, 2)$ , the posterior distributions of  $t_1$  and  $t_2$  will be multi-modal, which leads to non-identifiability. The third model setting treats the location of the stationary points as random and unknown and, furthermore, assumes that there is one stationary point only,  $t$ , with  $t \sim Unif(0, 2)$  as the prior distribution. This is the *single-DGP* model. As previously remarked, imposing one stationary point results in curves with at least one stationary point. This strategy, therefore, avoids the issue of mis-specifying the number of stationary points by letting the model learn number and locations of the stationary points. Results below show how single-DGP results in accurate estimation performance even in the case of multiple stationary points.

Figure 3 shows true and estimated regression functions, and corresponding 95% credible intervals, for one simulated dataset, under oracle, multiple and single DGP and a standard GP model. Credible intervals were obtained by conditional simulation, that is, by sampling a large number of values from the posterior distribution of  $t$  and, jointly, a large number of realizations of  $f$  from the GP model, conditioning upon the data and the estimated model parameters  $\theta$ . Although the estimated curves are pretty similar under the different scenarios, the credible intervals of oracle-DGP are narrower, especially where the true function is significantly increasing or decreasing (see for example  $x = 1$  with  $|f'(1)| = 1.74$  and  $x = 1.45$  with  $|f'(1.45)| = 0.047$ ). This result is of course expected, given that this setting assumes full knowledge of the number and locations of the stationary points. Multiple-DGP and single-DGP both result in slightly wider credible intervals, due to the uncertainty on the locations of the stationary points. A similar result is obtained with standard GPR.

In order to further assess estimation performances, we calculated root mean squared errors (RMSE) between the true regression function and the estimated curves, as a function

of  $x$ , averaged across the 100 simulated datasets, as  $\text{RMSE}(x_i^*) = \sqrt{\frac{\sum_{l=1}^{100} (f(x_i^*) - \hat{f}_{(l)}(x_i^*))^2}{100}}$ , with  $\hat{f}_{(l)}(x_i^*)$  the Bayes estimate of  $f$  at the test input  $x_i^*$  for the  $l$ -th dataset. Plots of the RMSE under the different settings are shown in Figure 2. In the same figure, as an additional comparison, we report results we obtained by applying a two-step frequentist method proposed by Song et al. (2006) that first employs nonparametric kernel smoothing (NKS) to estimate the curve derivatives and then finds the stationary points as those points at which the first derivative of the curve is zero. Results in Figure 2 confirm the superior performance of oracle DGP, with single and multiple DGP performing comparably to standard GPR. They also show the DGP methods generally have lower RMSE across locations of  $x$  than NKS.

[Figure 2 about here.]

[Figure 3 about here.]

Unlike standard GPR, multiple and single DGP models produce estimates of the location of stationary points in addition to the estimated curves. The bottom row of Figure 3 shows the posterior distribution of  $t$  from multiple-DGP and single-DGP obtained with the SEM algorithm. We note in particular that the distribution of  $t$  in the single-DGP setting is bimodal even through this setting assumes one stationary point. Vertical lines show the location of the true stationary points. These are correctly identified in both settings, even though some little densities can be observed near  $x = 0$  or  $2$  and result in wider credible intervals of  $f$  around the boundaries.

Point estimates of the stationary points can be obtained from the posterior distributions of  $t$ . Here we use as posterior summary the highest posterior density (HPD) interval, that not only provides a Bayesian credible interval for  $t$  but also gives a natural way to estimate the number of stationary points  $M$  as the number of discrete segments that compose the HPD interval. From a practical point of view, empirical estimates of the HPD interval for  $t$  can be

calculated as follows: Given the posterior samples of  $t$ , one can obtain the estimated density of  $t$ , say  $g(t)$ , and then the  $100(1 - \alpha)\%$  HPD interval is the subset  $C(g_\alpha)$  of  $\mathcal{X}$  such that  $C(g_\alpha) = \{t : g(t) \geq g_\alpha\}$  where  $g_\alpha$  is the largest constant such that  $P(t \in C(g_\alpha)) \geq 1 - \alpha$ . Alternatively, to avoid conditioning on an empirical point estimate of  $\boldsymbol{\theta}$ , one may implement an MCMC algorithm to draw posterior samples of  $\boldsymbol{\theta}$  and then draw posterior samples of  $t$  and  $f$ , conditional on such samples. Given the HPD interval, an estimate of the  $j$ -th stationary point is derived as the maximum a posteriori (MAP) estimate calculated as the mode of the  $j$ -th segment identified by the HPD interval. For our single-DGP model, the empirical 95% HDP intervals averaged over 100 simulated data were  $(0.377, 0.570)$  for  $\hat{t}_1$  and  $(1.568, 1.902)$  for  $\hat{t}_2$ . Furthermore, root mean square errors (RMSE) between the true and estimated stationary points, averaged over the 100 simulated datasets as  $\text{RMSE}(\hat{t}_j) = \sqrt{\frac{\sum_{l=1}^{100} (\hat{t}_j^{(l)} - t_j)^2}{100}}$ , with  $\hat{t}_j^{(l)}$  the estimate of  $t_j$  in the  $l$ -th simulated data set, were  $\text{RMSE}(\hat{t}_1) = 0.0384$  and  $\text{RMSE}(\hat{t}_2) = 0.0445$ , demonstrating that the single-DGP approach with HDP-based estimation provides high estimation accuracy. As for comparison with NKS, let  $\hat{t}_1^{(l)}$  and  $\hat{t}_2^{(l)}$  be the stationary points located in  $0 < x < 1$  and  $1 < x < 2$ , respectively, for the  $l$ -th data set. Then the RMSE of  $\hat{t}_1$  and  $\hat{t}_2$  were 0.1410 and 0.1760 respectively.

Additional simulations can be found in the Supplementary Material, where we investigate the effect of the signal-to-noise ratio (SNR) and the sample size on the goodness of fit of the estimation. Results for small sample sizes and small SNRs show that, while GPR cannot capture the correct shape of the true function, providing derivative information enhances estimation performance, in situations where the true function has some stationary points. At the request of a reviewer, we evaluated the effect of the choice of the kernel function on the methods performance by repeating the simulations using a Matérn kernel. While this function is not strictly differentiable everywhere, it does admit weak derivatives. Results are reported in the Supplementary Material.

#### 4. ERP Data Analysis

Event-related potentials (ERPs) are electrical potentials that represent electroencephalography (EEG) brain signals recorded in response to specific stimuli. ERP signals measured from EEG experiments have become a common tool in psychological research and neuroscience, due to their ability to provide information about a broad range of cognitive and affective processes. In a typical EEG experiment, to increase signal-to-noise ratio, stimuli are applied repeatedly and the resulting ERP waveforms are averaged across multiple trials for each subject and, often, across multiple subjects (Luck, 2012). A primary focus of ERPs analysis is to estimate the amplitude, i.e. magnitude (in microvolts) and the latency, i.e. position in time (in milliseconds, ms) of specific components of the ERP waveform, identified with the characteristic “peaks” and “dips” of the curve (see top left plot of Figure 4).

According to current best practices in ERP methodology, the identification of components is achieved by visual inspection of the grand-averaged ERP curve (average of all the subjects’s data) and constrained by previous findings in the literature using similar experimental designs (Luck, 2005, 2012). Then, the peak latency and the average or peak amplitude for that component is estimated within each subject. This is achieved by within subject averaging and then component estimation. Component latency is estimated as the point where the within subject curve reaches maximum amplitude, or where the component reaches half the area under the curve. When latency is not used, amplitude is typically estimated as the average amplitude across an entire component, with all points in the interval of the component contributing equally. This is, of course, unwise, since the value of interest is often the magnitude of the response, but uncertainty on how to measure this makes it necessary to use a broader interval to ensure all of the component is captured. It is desirable, then, to first generate a better single estimate of when the latency of peak amplitude for a component was reached, and then for that estimate to form the basis for the

selection of the time points at which amplitude is estimated. In this section we show how our proposed method can be employed to estimate smooth ERP curves and automatically identify characteristic components and their latencies through the detection of the stationary points of the curves. Unlike exploratory methods that rely on visual inspection of the curves, our method provides uncertainty quantification on the estimated quantities, in the form of HPD intervals. Furthermore, by explicitly accounting for error in the data, we avoid the excessive averaging which is routinely done to obtain smooth curves.

#### 4.1 *Experimental study*

We use data from an experiment performed at Rice University on speech recognition. Our ability to recognize speech from a complex acoustic signal depends on merging bottom-up sensory information with top-down expectations about what we are hearing. The goal of the experiment was to determine whether or not early stages of speech perception are independent of top down influences. In our analysis we consider data from two lexical biasing trial conditions (voiced vs unvoiced), with the aim of investigating the effects of lexicality on phoneme identification, specifically whether the identification is biased towards phonemes which form familiar words. Each experiment yielded a total of 2304 trials and EEG was continuously recorded during the task. More details on the experimental design and on the pre-processing of the EEG signals can be found in the Supplementary Material. In this paper, we analyze data from 11 college-age students and 11 older controls. Difficulties in perceiving speech, especially in noisy environments, is a common problem in aging (Pelle and Wingfield, 2016). Some age-related differences might be attributable to a general slowing of the cortical processes that comes with age, which would lead to the prediction that the ERP components associated with speech perception have longer latencies in older adults than in younger adults (Tremblay et al., 2003). By investigating younger and older people separately in this paradigm, we can better understand how early cortical responses to speech stimuli

change with age. Figure 4 shows the ERP waveform time-courses for each of the subjects, averaged over all trial conditions and 6 electrodes.

Typical analyses of ERP data use averaged ERP waveforms over a window of interest and a given condition to calculate magnitudes and latencies of specific components. For example, in Noe and Fischer-Baum (2020) the authors argue for the so called N100 component to be of interest, as this captures phonological (syllable) representation. This component is identified by the latency of the negative deflection, or dip, that typically characterizes the ERP signal in the time interval [60, 130]ms, after the onset of the stimulus (see Figure 4 ). For our analysis, we considered a larger time window that comprises the interval [50, 250]ms, containing 101 observation points, to include a second ERP feature of interest, the so called P200, an auditory component that represents some aspect of higher-order perceptual processing, modulated by attention, and that typically peaks at around 200 ms. Recent electrophysiological investigations using other imaging modalities have identified the time window around the P200 as potentially critical for processing higher-order speech perception processes (Leonard et al., 2016). Given the goal of the study, and the P200s potential role in speech perception processes, this is also an ERP component of interest. The ERP waveforms for the two (voiced vs unvoiced) lexical biasing trial conditions, averaged across young and older subjects, are shown in the lower plots of Figure 4. Although averaging across subjects leads to smoother ERP waveforms, the subject-specific variability observed in the subject-level ERP waveforms is washed out, and the information about subject-level ERP is lost.

[Figure 4 about here.]

## 4.2 Results

Given that we have available subject-level data on multiple subjects, we fit our GP regression model (1) - (3) as  $y_{i,s} = f_s(x_i) + \epsilon_{i,s}$ , with  $\epsilon_{i,s} \sim N(0, \sigma^2)$  and  $f_s(\cdot) \sim GP(0, k(\cdot, \cdot; \tau, h))$ , subject to  $f'_s(t_{m_s, s}) = 0$  for  $m_s = 1, \dots, M_s$ , with  $s = 1, \dots, S$  indicating the subject, and



$i = 1, \dots, n$  the time points. We assume that subjects share the same set of time points  $\{x_i\}_{i=1}^n$ , same covariance kernel and common parameters  $(\sigma, \tau, h)$ , while allowing subject-level stationary points  $t_{m,s}$ . We specify noninformative priors on  $\tau^2$  and  $h$ . Within each group of subjects, older and young, we assume a common error variance  $\sigma^2$  with an IG prior specified to match the empirical moments calculated based on the data on all subjects. For the prior of  $t$ , we use our knowledge that the occurrence of the N100 and P200 components is likely happening in the middle part of the chosen interval for analysis and specify a Beta(3, 3) distribution. When such prior knowledge is available, a Beta distribution is a more convenient choice than the uniform prior, as it avoids a potentially inflated density around the end points of the time courses. From our analysis, we obtain fitted ERP curves, for each subject, together with posterior distributions of their stationary points.

[Figure 5 about here.]

Figure 5 shows the 95% HPD regions of the posterior distributions of  $t$ . Results are given for older and young subjects, separately. Furthermore, for each group, separate analyses were performed by considering all the data first, and then by separating voiced and unvoiced biasing trial conditions. These plots show substantial subject-level variability, which is lost in the data averaging process. The observed variation in the location of the stationary points, i.e. the latencies of ERP components, clearly indicates subject-specific effects. Furthermore, few subjects show HPDs with multiple short intervals, suggesting possible outliers.

As a further validation, we used the R package *Rmixmod* to fit Gaussian mixtures with two components to the posterior samples of  $t$  obtained from the E-step of the SEM algorithm. We set a maximum of 50 iterations and used several short runs of the EM algorithm, launched from random positions, each stopping when the log-likelihood increment is smaller than a threshold (which we set to 0.001). Table 1 reports the estimated mean components, averaged across subjects, with averaged standard deviations. Averaged means and 95% CIs, calculated

as (mean  $\pm$  1.96 std), are reported in Figure 5. Results show clear latency differences between older and younger adults in both the N100 and the P200, with the N100 peak slowed by approximately 10ms difference in the N100 and 22ms difference in the P200. This supports the conclusion that at least some of the differences between older and younger adults in speech perception can be attributed to the speed of cortical processing of speech sounds.

Figure 5 shows greater variability in the timing of ERP components among older adults than younger adults, particularly in the timing of the P200 components. These differences can have enormous consequences on conclusions that we can draw from the standard method for analyzing ERP data. For example, the standard approach would be to select a window around a peak identified from globally averaged data, calculate the amplitude of that component in that region, and then compare between groups. Given the greater variability in the timing of the peaks for the older adults, we likely would find that older adults show a smaller amplitude than younger adults. However, we may not reach the same conclusion if we calculated amplitude on the basis of each individual participants peak-latency, as our method allows. Alternatively, we may find no differences between groups with the standard approach, when in fact the older adults consistently show a larger amplitude in their individual waveforms. Furthermore, since older adults are much more variable in their speech perception abilities than younger adults, this approach could be used to identify latencies of different components at the individual subject level and relate those latencies to behavioral differences.

Overall, our work clearly shows the need of model-based approaches for ERP data analysis that can identify subject-specific component latencies and amplitudes in a non-subjective, quantitative way. Our approach, in particular, constitutes a significant development over traditional approaches that arbitrarily average together subjects with different numbers of trials, different quality of data, and different latency for each component.

[Table 1 about here.]

## 5. Discussion

We have proposed a semiparametric Bayesian model to efficiently infer the locations of stationary points of a nonparametric function. The approach uses Gaussian processes as flexible priors for the underlying function while imposing derivative constraints to control the function's shape via conditioning. We have developed an inferential strategy that intentionally restricts estimation to the case of at least one stationary point, bypassing possible mis-specifications in the number of stationary points and avoiding the varying dimension problem that often brings in computational complexity.

We have illustrated the proposed methods using simulations and an application to event-related potentials (ERP). By applying our approach to data collected from younger and older adults during a speech perception task, we have demonstrated how the time course of speech perception processes change with age. Our results have clearly shown the advantage of model-based approaches to ERP data analysis. Extensions to multi-subject models that incorporate subject-level random effects via hierarchical modeling could be of practical relevance.

## References

- Adler, R. J. (1981). *The Geometry of Random Fields*, volume 62. SIAM.
- Gasser, T. and Molinari, L. (1996). The analysis of EEG. *Statistical Methods in Medical Research* **5**, 67–99.
- Ghosal, S. and van der Vaart, A. (2017). *Fundamentals of Nonparametric Bayesian Inference*. Cambridge University Press, Cambridge.
- Hajcak, G., Klawohn, J., and Meyer, A. (2019). The utility of event-related potentials in clinical psychology. *Annual review of clinical psychology* **15**, 71–95.
- Hasenstab, K., Scheffler, A., Telesca, D., Sugar, C. A., Jeste, S., DiStefano, C., and Şentürk, D. (2017). A multi-dimensional functional principal components analysis of EEG data.

- Biometrics* **73**, 999–1009.
- Hasenstab, K., Sugar, C. A., Telesca, D., McEvoy, K., Jeste, S., and Şentürk, D. (2015). Identifying longitudinal trends within EEG experiments. *Biometrics* **71**, 1090–1100.
- Hastings, W. (1970). Monte Carlo sampling methods using Markov chains and their application. *Biometrika* **57**, 97–109.
- Holsclaw, T., Sansó, B., Lee, H. K. H., Heitmann, K., Habib, S., Higdon, D., and Alam, U. (2013). Gaussian process modeling of derivative curves. *Technometrics* **55**, 57–67.
- Kallionp, R., Pesonen, H., Scheinin, A., Sandman, N., Laitio, R., Scheinin, H., and Valli, K. (2019). Single-subject analysis of n400 event-related potential component with five different methods. *International Journal of Psychophysiology* **144**, 14–24.
- Kim, A., Oines, L., and Miyake, A. (2018). Individual differences in verbal working memory underlie a tradeoff between semantic and structural processing difficulty during language comprehension: An ERP investigation. *Journal of Experimental Psychology: Learning, Memory, and Cognition* **44(3)**, 406–420.
- Leonard, M., Baud, M., Sjerps, M., and Chang, E. (2016). Perceptual restoration of masked speech in human cortex. *Nature communications* **7(1)**, 1–9.
- Luck, S. J. (2005). *An Introduction to the Event-Related Potential Technique*. The MIT Press.
- Luck, S. J. (2012). Event related potentials. In Cooper, H., Camic, P. M., Long, D. L., Panter, A. T., Rindskopf, D., and Sher, K. J., editors, *APA handbook of research methods in psychology, Vol 1: Foundations, planning, measures, and psychometrics*, pages 266–290. American Psychological Association.
- Noe, C. and Fischer-Baum, S. (2020). Early lexical influences on sublexical processing in speech perception: Evidence from electrophysiology. *Cognition* **197**, 1041–62.
- Parzen, E. (1962). On estimation of a probability density function and mode. *Ann. Math.*

- Statist.* **33(3)**, 1065–1076.
- Peelle, J. and Wingfield, A. (2016). The neural consequences of age-related hearing loss. *Trends in neurosciences* **39(7)**, 486–497.
- Rasmussen, C. E. and Williams, C. K. (2006). *Gaussian Process for Machine Learning*. The MIT Press.
- Song, P., Gao, X., Liu, R., and Le, W. (2006). Nonparametric inference for local extrema with application to oligonucleotide microarray data in yeast genome. *Biometrics* **62(2)**, 545–554.
- Tanner, D. (2019). Robust neurocognitive individual differences in grammatical agreement processing: A latent variable approach. *Cortex* **111**, 210–237.
- Tremblay, K., Piskosz, M., and Souza, P. (2003). Effects of age and age-related hearing loss on the neural representation of speech cues. *Clinical Neurophysiology* **114(7)**, 1332–1343.
- Wang, X. and Berger, J. O. (2016). Estimating shape constrained functions using Gaussian processes. *Journal on Uncertainty Quantification* **4**, 1–25.
- Zhou, S., Giuliani, P., Piekarewicz, J., Bhattacharya, A., and Pati, D. (2019). Reexamining the proton-radius problem using constrained Gaussian processes. *Physical Review C* **99**, 055202.

## Supporting Information

Supplementary material is available at the Biometrics website on Wiley Online Library. Behavioral and ERP data used in this paper are published on PsyArxiv, hosted by OSF (at <https://osf.io/c7k4s/>), with DOI: 10.17605/OSF.IO/C7K4S. R code to recreate results on simulated and real data can be found at <https://github.com/chenghanyustats/DGP>.

*Received ... .. Revised ...*

*Accepted ...*

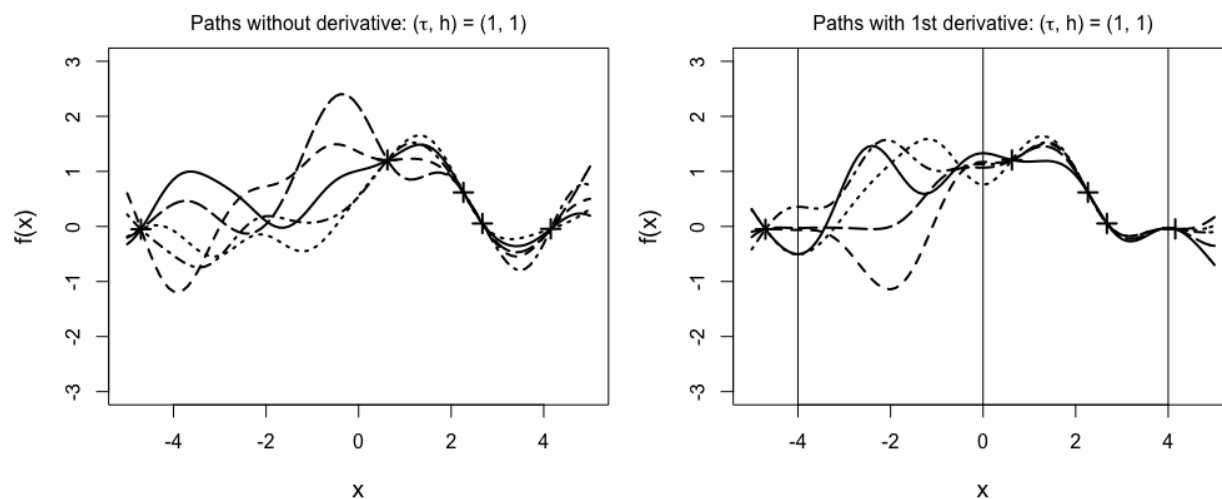


**Figure 1.** Sample paths from a Gaussian process with (right) and without (left) first order derivative information. A squared exponential kernel (4) with parameters  $\tau = 1$  and  $h = 1$  was used. The left-hand panel shows sample paths from a standard GP with input values randomly chosen from  $[-5, 5]$ , indicated with plus signs in the plot, while the right-hand panel shows sample paths from a DGP with stationary points  $t_1 = -4, t_2 = 0,$  and  $t_3 = 4,$  indicated with vertical lines in the plot. As expected, when the derivative constraints are added to the process, all curves have derivatives equal to zero at  $t_m, m = 1, 2, 3,$  but each curve generally takes its own values at  $t_m, m = 1, 2, 3.$

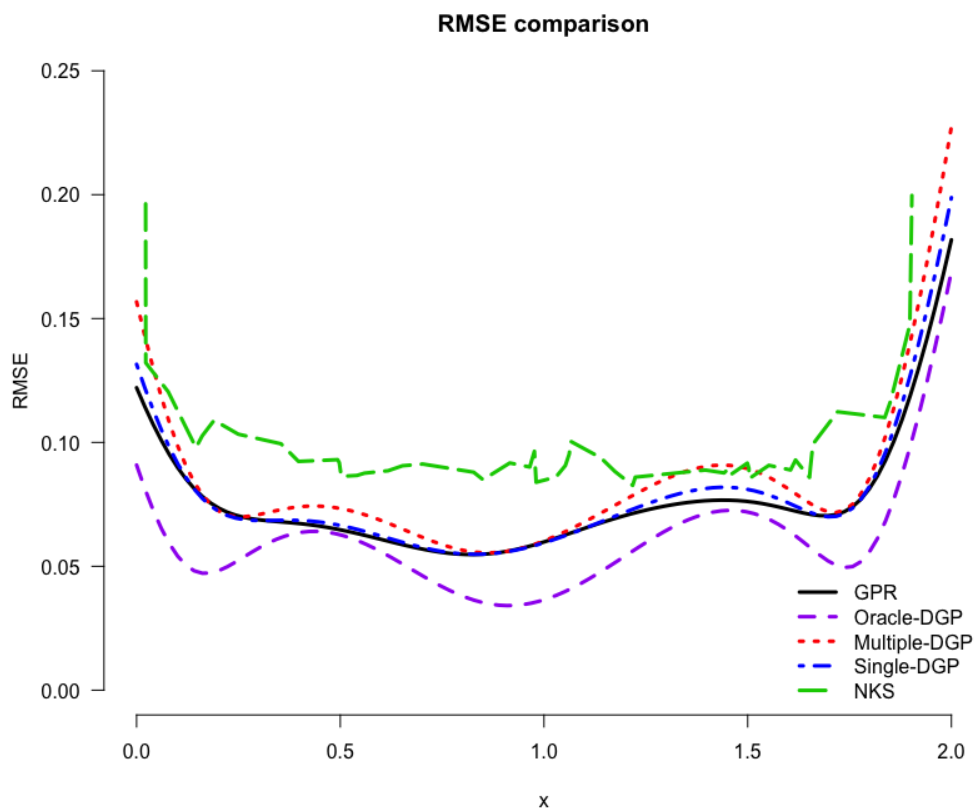


**Figure 2.** Simulated data. Root mean squared errors (RMSE) between the true regression function and the estimated curves, as a function of  $x$ , averaged across the 100 simulated datasets, for standard GPR, three different DGP models (oracle, multiple and single), as described in the text, and the NKS method of Song et al. (2006). The GPR and DGP methods use the test input  $x_i^*$  while NKS uses the original input  $x_i$ .

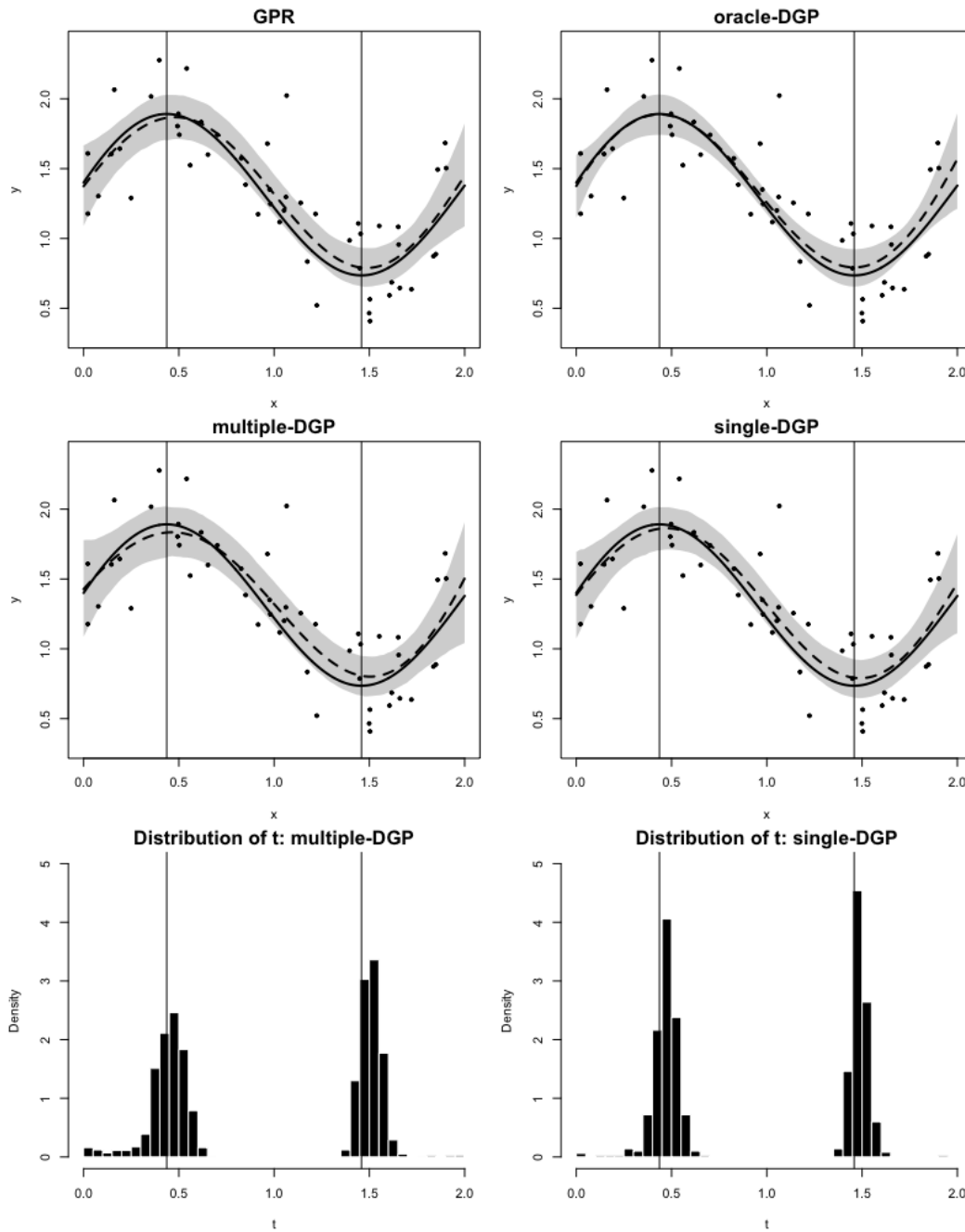


**Figure 3.** Simulated data. *Top two rows:* Estimated curves for one simulated dataset under different models: A standard GPR model and three different DGP models (oracle, multiple and single), as described in the text. The true regression function is shown as a solid line and the estimated curves as dashed lines. Dots indicate input values. *Bottom row:* Posterior distributions of  $t$ , for single and multiple DGPs, with vertical lines indicating the locations of the true stationary points.



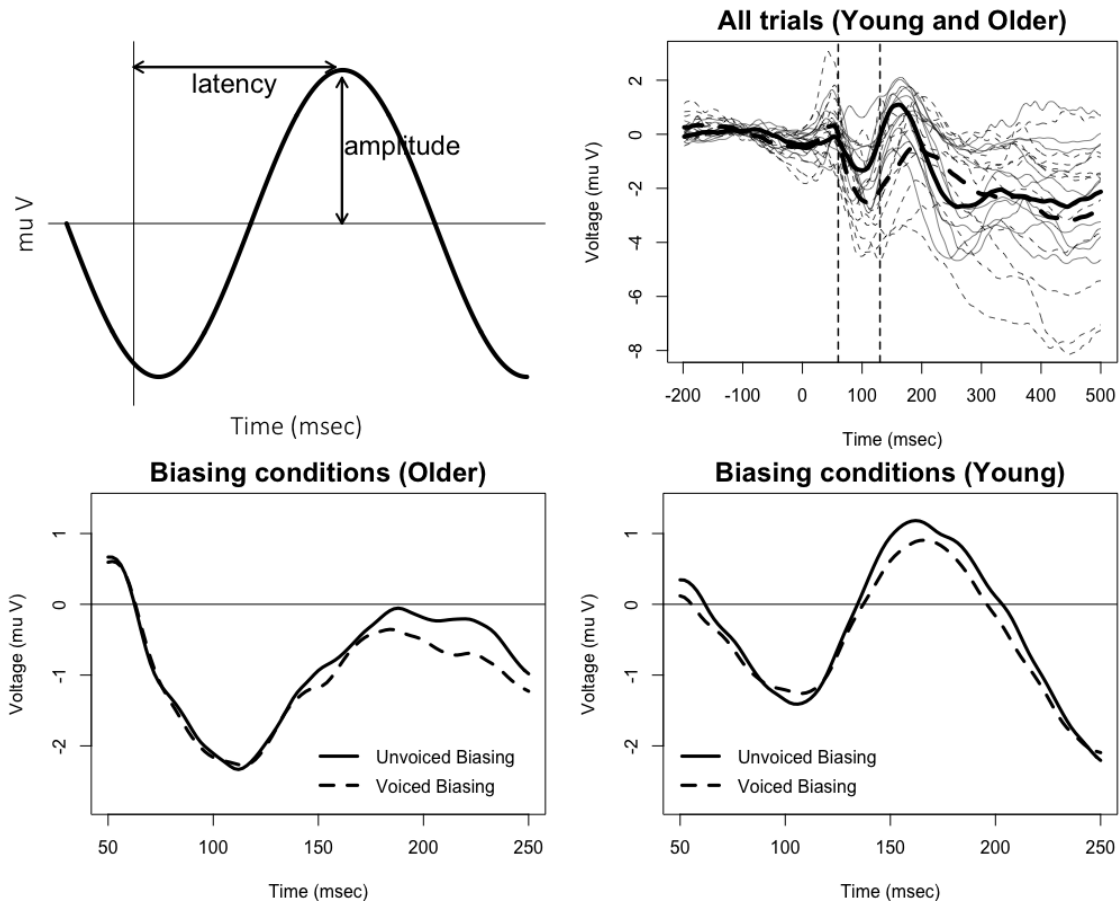


**Figure 4.** ERP Data Analysis: *Top left:* Illustration of amplitude and latency of characteristic components of an ERP signal. *Top right:* Subject-level ERP waveforms, averaged over all trial conditions. The continuous and dashed thick curves are the benchmark ERP averaged across young and older subjects, respectively. The 0ms time, which corresponds to time point 100, is the start of the onset of sound. Points 101 - 350 represent the time the stimulus is played. The N100 component of interest is the amplitude of the dip characterizing the signal in the time window between the vertical dashed lines. *Bottom plots:* ERP waveforms averaged across older and young subjects, for the two (voiced vs unvoiced) lexical biasing trial conditions of interest.

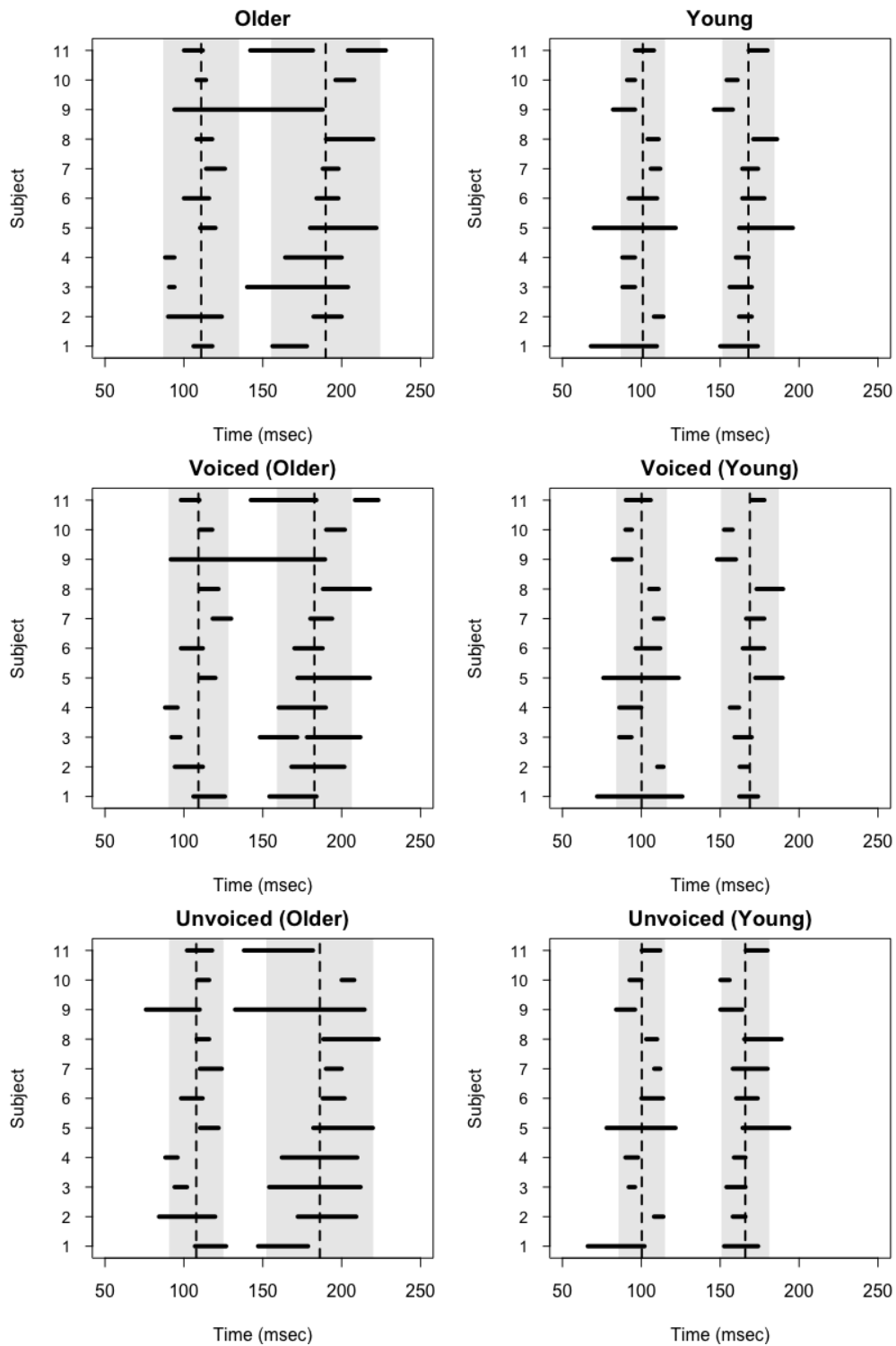


**Figure 5.** ERP Data Analysis: *Left column:* 95% HPD regions of the posterior distributions of  $t$  for the older group, for all subjects and for the voiced and unvoiced biasing trial conditions. *Right column:* 95% HPDs regions of the posterior distributions of  $t$  for the young subjects group. In all plots, the dash vertical lines indicate the posterior means obtained by fitting a Gaussian mixture to the posterior samples of  $t$ , averaged across subjects, and the 95% CI calculated as  $(\text{mean} \pm 1.96 \text{ std})$  and shown as shaded areas.

Group	$\hat{t}_1$	$\hat{t}_2$
young	100.97 (7.16)	167.87 (8.44)
voiced (young)	100.17 (8.20)	168.82 (9.34)
unvoiced (young)	100.30 (7.51)	165.91 (7.75)
older	110.95 (12.26)	189.85 (17.65)
voiced (older)	109.24 (9.70)	182.69 (12.12)
unvoiced (older)	107.85 (8.80)	186.15 (17.29)

**Table 1**

*ERP Data Analysis: Estimated mean components, from a Gaussian mixture model with two components fitted to the posterior samples of  $t$ , averaged across subjects, with averaged standard deviations in parentheses.*